Int. J. Electrochem. Sci., 11 **(2016)** 3727 - 3737

International Journal of
ELECTROCHEMICAL
SCIENCE
www.electrochemsci.org

Synthesis of UV-Cured Hyperbranched Polyurethane Acrylate Coatings and Its Corrosion Resistance Revealed by Electrochemistry

Jin Cui[1,2], *Yihe Zhang*[1,*], *Xiaoyong Hu*[2], *Paul K. Chu*[3], *Falong Wang*[2], *Xinke Wang*[1], *Yuqing Xu*[2]

[1] Beijing Key Laboratory of Materials Utilization of Nonmetallic Minerals and Solid Wastes, National Laboratory of Mineral Materials, School of Materials Science and Technology, China University of Geosciences, Beijing, 100083, China
[2] School of Biological and Chemistry Engineering, Guangxi University of Science and Technology, Liuzhou 545006, China
[3] Department of Physics and Materials Science, City University of Hong Kong, Tat Chee Avenue, Kowloon, Hong Kong, China
[*]E-mail: zyh@cugb.edu.cn

Received: 6 December 2015 / *Accepted:* 19 February 2016 / *Published:* 1 April 2016

First generation hyper-branched poly-ester-amine, second generation hyper-branched poly-ester-amine, and isophorone diisocyanate-2-hydroxyethylacrylate are first synthesized and the hyperbranched polyurethane acrylate oligomer is subsequently prepared with the second generation hyper-branched poly-ester-amine. Finally, the UV-cured hyper-branched coatings are produced with the hyper-branched polyurethane acrylate oligomers, methyl acrylate, 2-hydroxyethyl methacrylate, and photo-initiator 1173. The structure of the first generation hyper-branched poly-ester-amine, second generation hyper-branched poly-ester-amine, and hyper-branched polyurethane acrylate oligomers, and UV-cured coatings are characterized by FT-IR, TG, and SEM. The corrosion resistance of the hyper-branched coatings is studied electrochemically and compared to conventional coatings. The self-corrosion rate of conventional coatings drops from 28.022 mm/A to 17.468 mm/A and hyper-branched coatings from 28.022 mm/A to 8.061 mm/A. The hyper-branched coatings have very good thermal properties, corrosion resistance, as well as cross-linking density.

Keywords: UV-curing, hyperbranched coatings, polyurethane acrylate

1. INTRODUCTION

Because of rapid industrial development, environmental problems have become increasingly important [1]. Recently, the UV-curing technology has attracted considerable attention because of the

doi: 10.20964/110268

high reaction speed, environmental friendliness, as well as low energy consumption. Polyurethane acrylate (PUA) having good thermal and mechanical properties is widely used as an oligomer in UV coatings [2,3]. In the UV curing solvent-borne coats, reactive diluents are toxic and irritating with a strong odor and can volatilize easily thereby limiting their use in practice. Recently, water-borne UV curing coats have been developed to overcome the obstacles [4-7]. The use of water in water-borne UV-curable coatings decreases air pollution. Although water can control the film viscosity, there are still problems with water-borne coatings such as the small solid content and unsatisfactory producing efficiency. Hyper-branched polymers (HBPs) contain highly branched and polydispersed molecules [8]. HBPs have a unique structure resulting from a good deal of reactive end-groups. Thus, HBPs possess desirable properties; for instance, low melting point and viscosity, and easy functionalization compared with their linear counterparts [9-12]. There are interests in introducing HBPs to UV-curing systems. For example, Han et al. [13] synthesized HBP_2UA-HMPP by using the reaction between the hydroxy groups of $HBPE_2$ (second generation hyper-branched poly-ester-amine and IPDI–HEA and IPDI–HEMA with different ratios. The prepared oligomers showed good solubility in solvents such as dimethylformamide, dimethylacetamide, and dimethyl sulfoxide, and the coatings also had excellent thermal characteristics.

In this study, HBP_1-OH, HBP_2-OH, and IPDI-HEA are first synthesized and the HBPUA oligomers are is prepared with HBP_2-OH and IPDI-HEA. The UV-cured HBPUA coatings are then prepared with the HBPUA oligomers, MA (methyl acrylate), HEMA, and photoinitiator 1173. The structure of HBP_1-OH, HBP_2-OH, HBPUA oligomers, and UV-cured coating are characterized and the corrosion behavior of three types of carbon steel is studied and compared.

2. EXPERIMENTAL DETAILS

2.1 Materials

Pentaerythritol triacrylate (PETA), IPDI, HEA, HEMA, and methyl acrylate(MA) were provided by Tianjin Tianjiao Chemical Co. Dibutyltin dilaurate (DBTDL) was obtained from Jinan Yingyu Chemical Co. and diethanolamine (DEA) was purchased from Guangzhou Yinlin Chemical Co. Tetrahydrofuran (THF) was provided by Shanghai Jinjinle Co. and acetone was bought from Dongguan Zhongtian Chemical Co. Methylbenzene and methanol were purchased from Dongguan Qiming Chemical Co. and the photoinitiator 1173 was supplied by Shenzhen Haichengxingye Science and Technology Co. All the chemicals were used as received directly.

2.2 Characterization

The FT-IR analysis were conducted by a Nexus 550II spectrometer and scanned from 500 to 4000 cm^{-1}. The highest resolution is 0.1 cm^{-1}. The test was conducted in room temperature.

The 1H NMR analysis of HBP_1-OH and HBP_2-OH were conducted on a Bruker 250-MHz Spectrometer. Tetramethylsilane (TMS) and DMSO-d_6 were used as internal standard and solvents, respectively. The scanning frequency is 600 MHz.

The TG-DSC spectra of HBP_1-OH, HBP_2-OH, HBPUA coatings, and traditional PUA coatings were acquired on the Rigaku TSA-100 instrument at a constant heating rate 10 ℃/min between 0 ℃ and 800 ℃ under N_2 environment. Every sample weight roughly 10 mg.

The surface morphology of the HBP_1-OH, HBP_2-OH, HBPUA coatings, and traditional PUA coatings was examined on the S-4700 scanning electron microscope at 25 kV (accelerating voltage).

The corrosion behavior of three carbon steel samples: the first one coated with HBUA coatings, the second one coated with traditional PUA coatings, and the third one uncoated), which measured by three-electrode system (working electrode is the three carbon steel samples, counter electrode is Pt plate, and reference electrode is Ag/AgCl electrode), is determined by Nyquist plots and polarization curves. AC (alternating current) impedance testing frequency range from 100 kHz to 50 mHz, and AC signal is 5 mV. Before testing in 3.5% NaCl solution, the system always have 15 min under N_2 environment. Polarization curves were obtained under a 1 mV/s scan rate. All the measurement were proceeded in room temperature.

2.3 Preparation of HBP_1—OH

HBP_1-OH was synthesized according to Eq. 1. The flask was equipped with nitrogen inlet tube, magnetic stirring bar, and thermometer. DEA (0.12 mol) and PETA (0.03 mol) were dissolved in methanol (45 mL) at 35 °C for 36 h under stirring. After cooling to ambient temperature, the precipitate was filtered and vacuum dried to yield HBP_1-OH (Yield: 17.6 g, 80%).

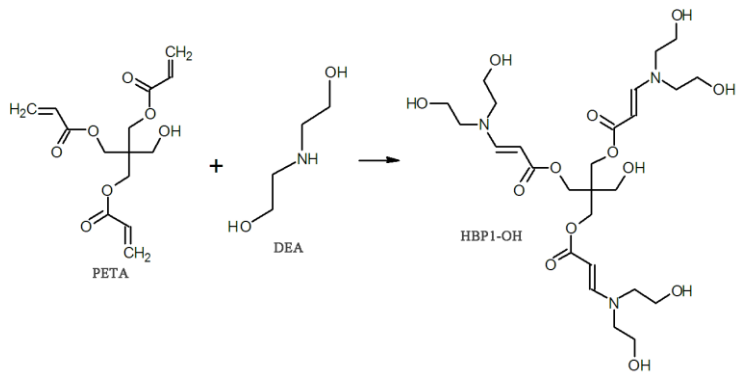

Equation 1. Synthesis of HBP_1-OH by PETA and DEA. Nitrogen atom of DEA reacted with carbon-carbon double bond of PETA to form tertiary amine group in HBP_1-OH.

2.4 Preparation of NNDAP

NNDAP (N,N–Diethyl–3–amine methyl propionate) was obtained according to Eq. 2. MA (42 g), DEA (34.4 g), and methanol (30 mL) were added to the flask with a magnetic stirring bar and

condenser for 4 h at 40 °C under stirring. NNDAP, a colorless liquid, was obtained by removing mehanol.

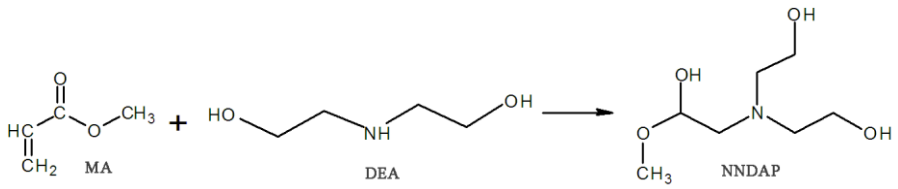

Equation 2. Synthesis of NNDAP by MA and DEA. Nitrogen atom of DEA reacted with carbon-carbon double bond of MA to form tertiary amine group in NNDAP.

2.5 Preparation of HBP$_2$-OH

HBP$_2$-OH was obtained from HBP$_1$-OH and NNDAP as described in Eq. 3. The flask was equipped with magnetic stirring bar, thermometer, and water separator. HBP$_1$-OH (5.8 g) was added and then NNDAP (8.61 g) and methanol (30 mL) were added dropwise to under stirring. After 6 h at 120 °C, HBP$_2$-OH was refined by fractional precipitation in a similar manner as HBP$_1$-OH. The yield of HBP$_2$-OH was 10.86 g (87%).

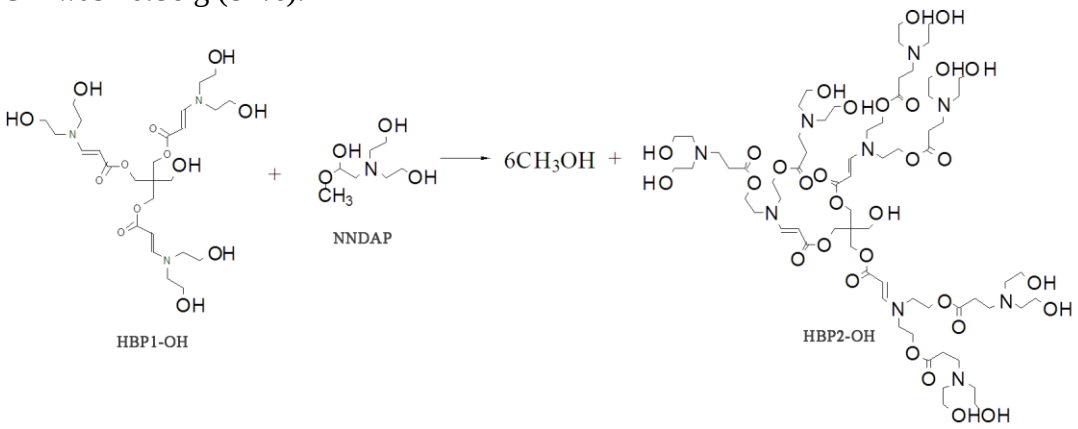

Equation 3. Synthesis of HBP$_2$-OH by HBP$_1$-OH and NNDAP. Hydrogen atom of HBP$_1$-OH reacted with methyl of NNDAP to form methanol in HBP$_2$-OH.

2.6 Preparation of IPDI-HEA

IPDI-HEA was sythesized according to Eq. 4. The flask was equipped with magnetic stirring bar, thermometer, and dropping funnel. DBTDL (0.1 g), IPDI (14.2 g), and acetone (45 mL) were added. HEA (7.4 g) was dissolved in *p*-hydroxyanisole (0.025 g) and then added dropwise to the reaction mixture at low temperature for 4 h under stirring. The mixture was maintained for about 12 h at 55 °C under stirring. The IPDI–HEA was obtained.

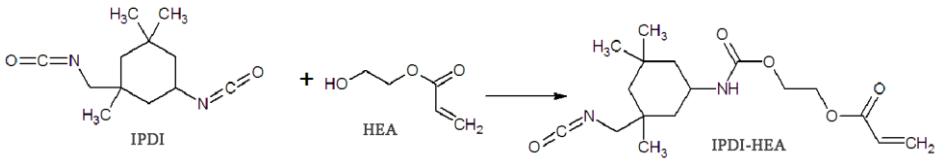

Equation 4. Synthesis of IPDI-HEA by IPDI and HEA. Carbonyl of IPDI reacted with hydroxyl of HEA to form ester linkage in IPDI-HEA.

2.7 Preparation of HBPUA oligomers

IPDI-HEA was added to HBP_2-OH (12.48 g) dissolved in THF (50 mL) at 65 °C for 9 h under stirring. After removing THF, HBPUA oligomers was obtained. The synthetic process is outlined in Eq. 5.

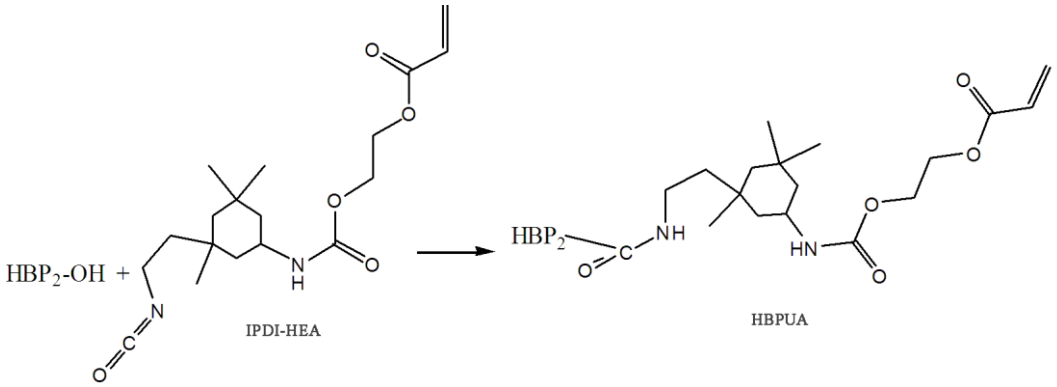

Equation 5. Synthesis of HBPUA by HBP_2-OH and IPDI-HEA. Carbonyl of IPDI-HEA reacted with hydroxyl of HBP_2-OH to form ester linkage in HBPUA.

3. RESULTS AND DISCUSSION

Fig. 1 shows the FT-IR spectra of HBP_1-OH, HBP_2-OH, and HBPUA oligomers. The spectrum of HBP_1-OH shows the characteristic bands of C=O at 3352 cm^{-1} (C=O stretching vibration), C—O—C at 1419 cm^{-1}, C—N at 1269 cm^{-1}, C—O at 1129 cm^{-1}, C=C—H at 1017 cm^{-1} (C—H in-plane bending vibration), C—N at 1297 cm^{-1} (C—N stretching of C—N=). The characteristic band of —N— signifies successful synthesis of HBP_1-OH.

The spectrum of HBP_2-OH shows the characteristic bands of C—H at 2960 and 2850 cm^{-1}, C—O—C at 1419 cm^{-1}, C—N at 1269 cm^{-1}, C—O at 1129 cm^{-1}, C=C—H at 1017 cm^{-1} (C—H in-plane bending vibration), C—N= at 1297 cm^{-1}, C=O at 3352 cm^{-1}. The absorbed dose of C=O of HBP_2-OH is twice that of HBP_1-OH because one HBP_1-OH molecule only has one C=O, but one HBP_2-OH molecule has two C=O. The results indicate successful synthesis of HBP_2-OH.

The spectrum of the HBPUA oligomers shows the characteristic bands of C=O at 3335 cm^{-1}, O=C—C=C— at 1662 cm^{-1}, 1406 cm^{-1}, and 810 cm^{-1} (C=C vibration), benzene ring elastic vibration

at 3068 cm^{-1}, C=O at 1713 cm^{-1}, —C—O at 1191 cm^{-1}, and N—H at 1537 cm^{-1}. The appearance of the absorption bands of NCO (2269 cm^{-1}) illustrates NCO and OH reacted completely.

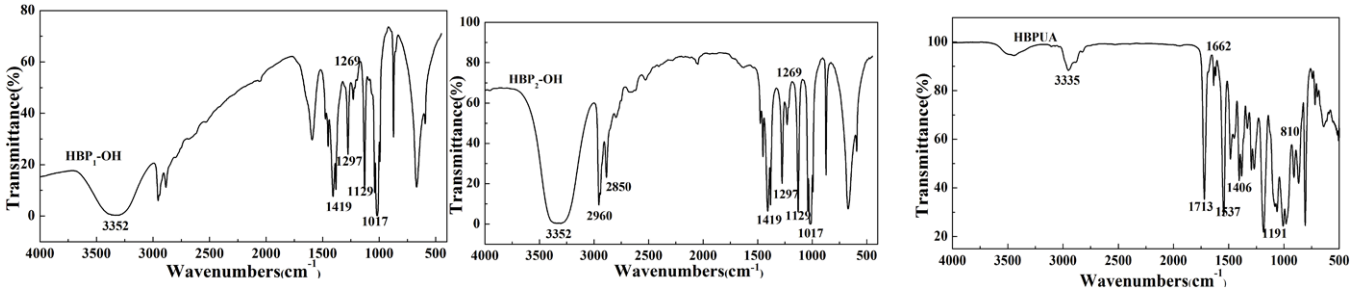

Figure 1. FT-IR spectra of HBP_1-OH (the left), HBP_2-OH (the centre), and HBPUA oligomer (the right). The characteristic bands of C=O at 3352 cm^{-1} in FT-IR spectra of HBP_1-OH and HBP_2-OH are different. The absorption of C=O stretching vibration in HBP_2-OH is less than HBP_1-OH.

Molecular structure of HBP_1-OH and HBP_2-OH are characterized by ^1H NMR equipment. Fig. 2 shows the ^1H NMR spectrum of HBP_1-OH and HBP_2-OH. Both spectra show two peaks at 3.46 ppm and 4.69 ppm. The peak at 3.46 ppm is ascribed to the C—H protons and that at 4.69 ppm arises from the O—H protons. The peak height of HBP_2-OH is 3.46 ppm whereas that of HBP_1-OH is 3:2 compared to HBP_2-OH at 4.69 ppm and HBP_1-OH being 3:1. In theory, the two radios are 13:7 and 110:26, respectively. The deviation from theory is because a small amount of HBP_1-OH still exists in HBP_2-OH.

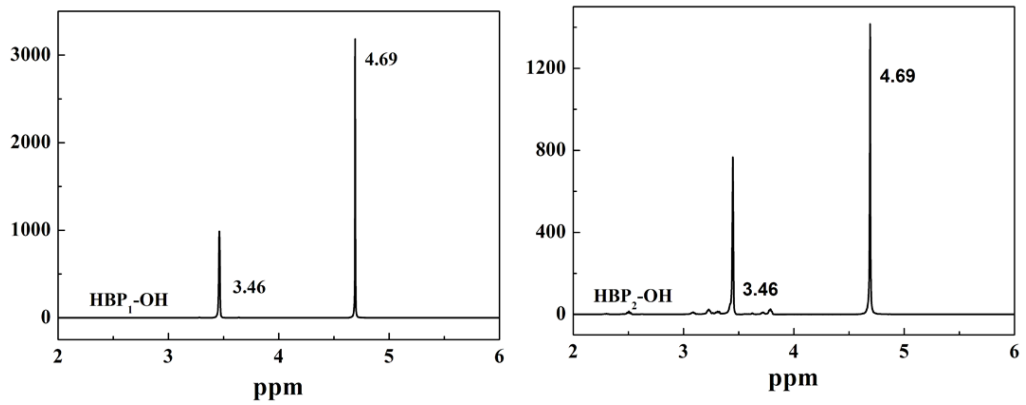

Figure 2. ^1H-NMR spectra of HBP_1-OH (the left) and HBP_2-OH (the right). Both HBP_1-OH and HBP_2-OH have only two peaks. Both peaks at 3.46 and 4.69 ppm in HBP_1-OH is less than HBP_2-OH.

Thermostability of polymer decided by cohesive energy of chemical bond, crosslinking level and heat conductivity[14]. The thermal characteristics of HBP_1-OH, HBP_2-OH, HBPUA coatings, and PUA coatings are evaluated by raising the temperature from 0 to 800 °C at a rate of 10 °C/min. As is shown in Fig. 3, the initial decomposition temperatures of HBP_1-OH, HBP_2-OH, HBPUA coatings,

and PUA coatings are 20 °C, 19 °C, 21.8 °C, and 26°C, respectively. Decomposition of polymer start with breaking in the weakest bond[15]. The decomposition temperatures of 5% weight loss are 209 °C, 238 °C, 245 °C, and 158 °C, decomposition temperatures of 10% weight loss are 236 °C, 261 °C, 327 °C, and 213 °C, and the tiptop temperatures are 350 °C, 320 °C, 350 °C, and 450 °C, respectively. With temperature rising, bond liberation degree increased, crosslinking level decreased and heat conductivity enlarged[16]. The results indicate that the thermostability of HBP_2-OH is better than that of HBP_1-OH and HBPUA is better than PUA since the former has a larger molecular weight. With regard to the HBPUA and PUA coatings, the weight loss below 300°C is because the volatilization of small molecular compounds such as the solvent. The weight loss between 300°C and 450°C is because the decomposition of crosslinked terminal urethane-acrylate groups and that at over 450 °C stems from decomposition of the benzene ring.

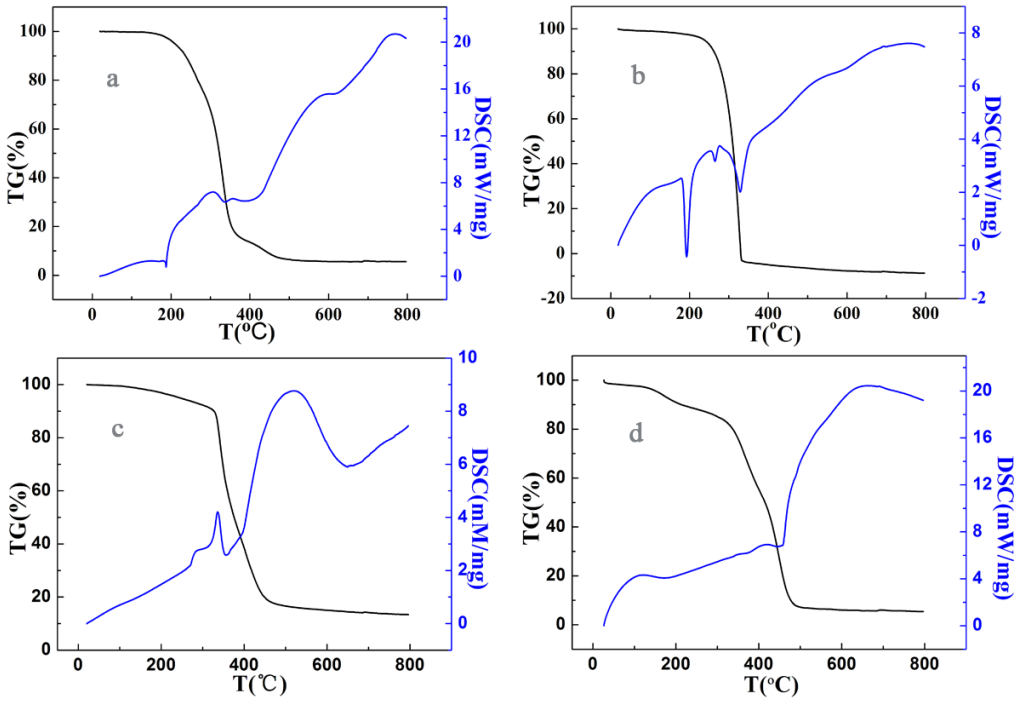

Figure 3. TG-DSC curves: (a) HBP_1-OH, (b) HBP_2-OH, (c) HBPUA coating, and (d) PUA coating. Both curves in HBP_1-OH and HBP_2-OH indicate the products' weight changed from 200°C to 330°C, while HBPUA coating and PUA coating changed from 300°C to 420°C.

As shown in Fig. 4, HBP_1-OH manifests as a particle cluster and HBP_2-OH looks like blobs. This is because the latter has larger molecular weight and so the intermolecular force is larger leading to steric effects. The surface of PUA present many small cracks and several large cracks, which are ductile fractures[17]. Morphological structure have both soft segment and hard segment. In HBPUA and PUA morphological structure, acrylate serve as soft segment, while urethane serve as hard segment[18,19,20,21]. The HBPUA coating is more uniform than the PUA coating which also has more cracks. This may be due to the formation of the cross-linking structure.

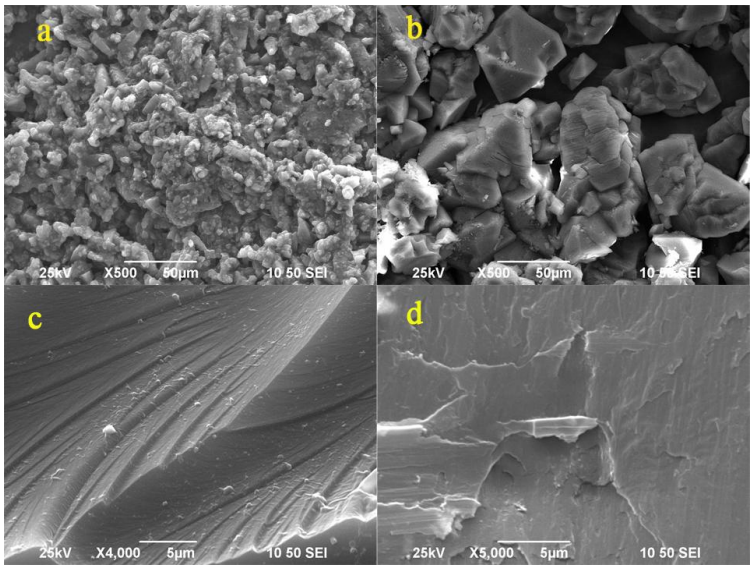

Figure 4. SEM micrographs: (a) HBP_1-OH, (b) HBP_2-OH, (c) HBPUA coating, and (d) PUA coating. Both HBP_1-OH and HBP_2-OH are powder, while HBPUA coating and PUA coating are films.

In Fig. 5, the Nyquist plots of three types of carbon steel under open circuit potential (OCV) in 3.5% NaCl solution have a semicircular shape, which were single dispersing capacitive loop[22]. It also be known as Sluyter plots. Top point fit the equation of $\tan\Phi=1$, while $\Phi=\pi/4$. Angular frequency (w) on top point is known as characteristic frequency (w*). It is possible to work out the capacitance (C) from radius (R) and characteristic frequency (w*), which formula is $C=1/(R\ w^*)$[23,24,25]. The smallest radius observed from the carbon steel Nyquist plot represents the worst corrosion resistance. After coating with the polymer, the redox potential larger than that of the carbon steel. The redox reaction occurs when the polymer is in contact with the carbon steel and the oxide covers and protects the carbon steel. The results also illustrate that the HBPUA coating has better corrosion resistance than traditional PUA coatings probably because of the later surface have more cracks, which allow corrosive medium across coatings in order to etch the substrate[26,27].

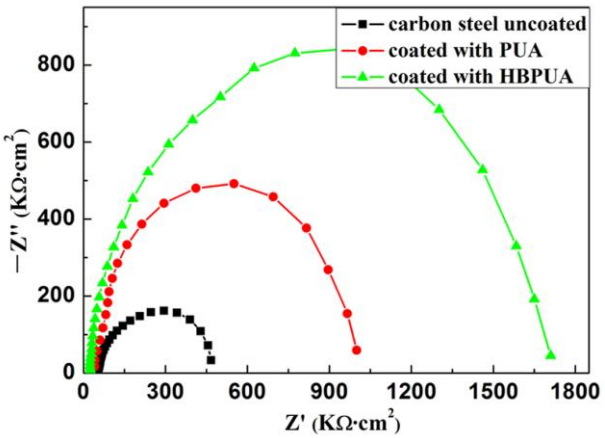

Figure 5. Nyquist plots of the three types of carbon steel.

As seen in Fig. 6 and Table 1, the self-corrosion current density of the carbon steel coated with the traditional PUA coating increases from -1.0403 V to -0.8351 V whereas that of HBPUA changes from -1.0403 V to 1.493×10^{-3} A/cm^2. The self-corrosion current potential of PUA drops from 2.395×10^{-3} A/cm^2 to 1.493×10^{-3} A/cm^2 and HBPUA from 2.395×10^{-3} A/cm^2 to 0.689×10^{-3} A/cm^2. The self-corrosion rate of PUA drops from 28.022 mm/A to 17.468 mm/A and HBPUA from 28.022 mm/A to 8.061 mm/A. The anodic Tafel slope of PUA increases from 0.181 V/dec to 0.211 V/dec, and cathodic Tafel slope increases from 0.269 V/dec to 0.341 V/dec, while HBPUA from 0.181 V/dec to 0.274 V/dec, and from 0.269 V/dec to 0.409 V/dec. The reason is that films coat on steel, which prevented steel from oxidation [28,29,30]. All Polarization curves of the three types of steel didn't have activation-passivation transition region. Because those electric potentials of cathodic reaction are higher than passive potentials [31]. It is clear that the HBPUA coating has better corrosion resistance than traditional PUA coatings due to the cross-linking and uniform structure.

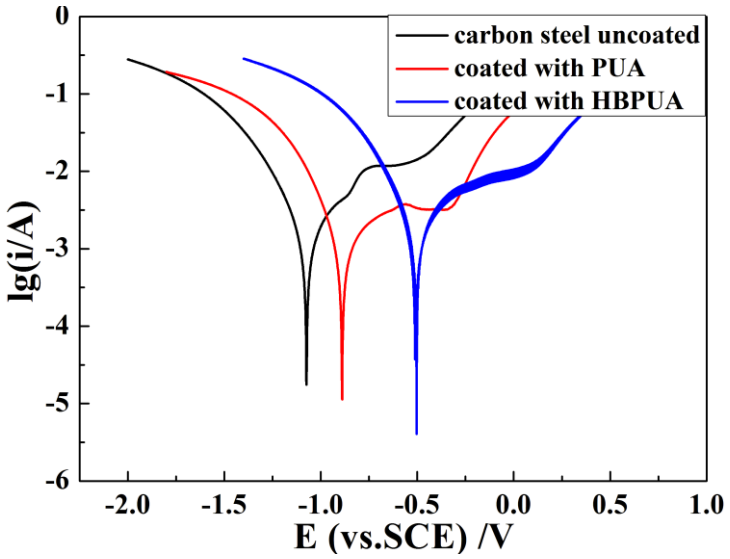

Figure 6. Polarization curves of the three types of steel.

Table 1. Self-corrosion current density, potential, rate and Tafel slopes.

Carbon steel	J_{corr} (A/cm^2)	E_{corr} (V)	V_{corr} (mm/A)	β_a(V/dec)	β_c(V/dec)
Uncoated	2.395×10^{-3}	−1.0403	28.022	0.181	0.269
Coated with PUA	1.493×10^{-3}	−0.8351	17.468	0.211	0.341
Coated with HBPUA	0.689×10^{-3}	−0.4952	8.061	0.274	0.409

4. CONCLUSION

HBP_1-OH, HBP_2-OH, and HBPUA are synthesized and characterized by FT-IR, ^{1}H NMR, TG, SEM, Nyquist plots and polarization curves. The thermostability of HBP_2-OH is better than that of

HBP_1-OH and the thermostability of HBPUA is in turn better than that of traditional PUA. The HBPUA coatings have better uniformity than the PUA coatings which also have more cracks. The self-corrosion rate of HBPUA is smaller than PUA. The HBPUA coatings have better corrosion resistance than traditional PUA coatings and our results indicate that the HBPUA coatings can be used as UV-cured coatings.

ACKNOWLEDGEMENTS
We acknowledge the support of School of Biological and Chemistry Engineering, Guangxi University of Science and Technology, Hong Kong Research Grants Council (RGC) General Research Funds (GRF) No. CityU 11301215, as well as City University of Hong Kong Applied Research Grant (ARG) No. 9667104.

References

1. E. S. Jang, S. B. Khan, J. Seo, Y. H. Nam, W. J. Choi, K. Akhtar and H. Han, *Prog. Org. Coat.*, 71 (2011) 36.
2. S. K. Asha, M. Thirumal, A. Kavitha and C. K. S. Pillai, *Eur. Polym. J.*, 41 (2005) 23.
3. R. Schwalm, L. Hauszling, W. Reich, E. Beck, P. Enenkel and K. Menzel, *Prog. Org. Coat.*, 32 (1997) 191.
4. C. Y. Bai, X. Y. Zhang, J. B. Dai and J. H. Wang, *J. Coat. Technol. Res.*, 5 (2008) 251.
5. J. Geurts, J. Bouman and A. Overbeek, *J. Coat. Technol. Res.*, 5 (2008) 57.
6. M. M. El-Molla, *Dyes Pigm.*, 74 (2007) 371.
7. B. U. Ahn, S. K. Lee, S. K. Lee, J. H. Park and B. K. Kim, *Prog. Org. Coat.*, 62 (2008) 258.
8. Q. Z. Gao, H. Q. Li and X. R. Zeng, *J. Coat. Technol. Res.*, 8 (2011) 61.
9. A. Blencowe, L. Davidson and W. Hayes, *Eur. Polym. J.*, 39 (2003) 1955.
10. M. Jin, R. Lu, C. Y. Bao, T. H. Xu and Y. Y. Zhao, *Opt. Mater.*, 26 (2004) 85.
11. E. Dzunuzovic, S. Tasic, B. Bozicb, D. Badic and B. Dunjic, *Prog. Org. Coat.*, 52 (2005) 136.
12. A. Asif, W. F. Shi, X. F. Shen and K. M. Nie, *Polymer*, 46 (2006) 11066.
13. W. S. Han, B. P. Lin, Y. H and X. D. Zhou, *Polym. Bull.*, 68 (2012) 729.
14. L. Kirmair, D. L. Seiler, A. Skerra, *Appl. Microbiol. Blot.*, 99 (2015) 10513.
15. X. M. Zhu, X. Y. Jiang, X. P. Ai, *Acs. Appl. Mater. Inter.*, 7 (2015) 24119.
16. Y. X. Han, H. Zhou, Y. Q. Wei, Y. J. Mei, H. Wang, *J. Mol. Liq.*, 211 (2015) 481.
17. Y. Y. Yang, G. H. Li, X. Y. Yu, H. L. Ding, Q. X. Zhang, N. Y. Wang, X. W. Qu, *Polym. Bull.*, 71 (2014) 9.
18. X. G. Zhang, B. Zhang, M. M. Sun, L. H. Li, L. Wang, C. L. Qin, *Pigm. Resin Technol.*, 43 (2014) 8.
19. Y. C. Chung, H. Y. Kim, J. W. Choi, B. C. Chun, *Macromol. Res.*, 22 (2014) 1115.
20. M. Alishiri, A. Shojaei, M. J. Abdekhodaie, H. Yeganeh, *Mat. Sci. Eng. C-Mater.*, 42 (2014) 763.
21. M. Shin, Y. Lee, M. Rahman, H. Kim, *Polymer*, 54 (2013) 4873.
22. M. Behpour, N. Mohammadi, E. Alian, *J. Iron Steel Res. Int.*, 21 (2014) 121.
23. S. J. Patil, A. C. Lokhande, C. D. Lokhande, *Mat. Sci. Semicon. Proc.*, 41 (2016) 132.
24. R. Zhou, T. Shao, M. D. G. Pascual, F. Smyth, L. P. Barry, *Ieee Photonic. Tech.*, 27 (2015) 2595.
25. J. Gong, M. Park, Y. Choi, H, Choi, M. Jeon, *J. Korean Phys. Soc.*, 67 (2015) 1899.
26. F. B. Ravari, A. Dadgareenezhad, *J. Chil. Chem. Soc.*, 58 (2013) 1853.
27. H. Singh, *Jom*, 67 (2015) 2564.
28. L. A. Jia, C. H. Liang, N. B. Huang, *J. Alloy. Compd.*, 656 (2016) 961.
29. Y. Sangeetha, S. Meenakshi, C. S. Sundaram, *Carbohyd. Polym.*, 136 (2016) 38.

30. M. Mobin, M. Rizvi, *Carbohyd. Polym.*, 136 (2016) 384.
31. A. Mohammad, N. E. Mojtaba, U. A. Saviour, *J. Adhes. Sci. Technol.*, 30 (2016) 89.